molecular
systems
biology

Reconstruction of the yeast Snf1 kinase regulatory network reveals its role as a global energy regulator

Renata Usaite[1,2], Michael C Jewett[1,3], Ana Paula Oliveira[1,4], John R Yates III[2], Lisbeth Olsson[1,5] and Jens Nielsen[1,5,*]

[1] Department of Systems Biology, Center for Microbial Biotechnology, BioCentrum-DTU, Technical University of Denmark, Lyngby, Denmark and [2] Department of Cell Biology, Proteomics Mass Spectrometry Labratory, The Scripps Research Institute, La Jolla, CA, USA
[3] Present address: Department of Genetics, Harvard Medical School, 77 Avenue Louis Pasteur, Boston, MA 02115, USA
[4] Present address: Institute for Molecular Systems Biology, ETH Zurich, Zurich 8093, Switzerland
[5] Present address: Department of Chemical and Biological Engineering, Chalmers University of Technology, Kemigarden 4, Gothenburg 412 96, Sweden
* Corresponding author. Department of Chemical and Biological Engineering, Chalmers University of Technology, Kemigarden 4, Gothenburg 412 96, Sweden.
Tel.: + 31 772 38 05; Fax: + 31 772 38 01; E-mail: nielsenj@chalmers.se

Highly conserved among eukaryotic cells, the AMP-activated kinase (AMPK) is a central regulator of carbon metabolism. To map the complete network of interactions around AMPK in yeast (Snf1) and to evaluate the role of its regulatory subunit Snf4, we measured global mRNA, protein and metabolite levels in wild type, Δ*snf1*, Δ*snf4*, and Δ*snf1*Δ*snf4* knockout strains. Using four newly developed computational tools, including novel DOGMA sub-network analysis, we showed the benefits of three-level ome-data integration to uncover the global Snf1 kinase role in yeast. We for the first time identified Snf1's global regulation on gene and protein expression levels, and showed that yeast Snf1 has a far more extensive function in controlling energy metabolism than reported earlier. Additionally, we identified complementary roles of Snf1 and Snf4. Similar to the function of AMPK in humans, our findings showed that Snf1 is a low-energy checkpoint and that yeast can be used more extensively as a model system for studying the molecular mechanisms underlying the global regulation of AMPK in mammals, failure of which leads to metabolic diseases.
Molecular Systems Biology **5**: 319; published online 3 November 2009; doi:10.1038/msb.2009.67
Subject Categories: metabolic and regulatory networks; signal transduction
Keywords: catabolic repression; metabolome; proteome; transcriptome

Introduction

AMP-activated kinases (AMPKs) are highly conserved among yeast, plants, and mammals and are central regulators involved in cellular development and survival (Polge and Thomas, 2007). Mammalian AMPK, for example, is a master regulator of energy control (Kahn *et al*, 2005). Its function is linked to metabolic and aging diseases and it is a key drug target against obesity and diabetes (Hardie, 2007a). Through homology studies, yeast AMPK (Snf1) has been used as a model to study human AMPK. For example, the upstream kinases of Snf1 (Elm1, Pak1, and Tos3) helped identify their mammalian counterparts, Lkb1 and CaMKK-β, that activate human AMPK (Hardie and Sakamoto, 2006).

The yeast Snf1 regulates carbon metabolism during growth on various carbon sources (Celenza and Carlson, 1986; Carlson, 1999). In a complex with its regulator Snf4 and scaffolding protein Gal83, Snf1 regulates the usage of alternative carbon sources through the transcription factors (TFs) Mig1 and Cat8 (Schuller, 2003). Two other Snf1 scaffolding proteins Sip1 and Sip2 determine distinct Snf1-substrate specificity, sub-cellular localization and function (Vincent *et al*, 2001).

There is, however, growing evidence that suggests a much broader role of Snf1 as a master regulator of carbon and energy metabolism. Genome-wide transcriptional profiling in yeast batch cultures has identified that active Snf1 is required for more than 400 of 1500 gene expression changes under glucose exhaustion (DeRisi *et al*, 1997; Young *et al*, 2003). At the level of protein interactions (BioGRID database) (Stark *et al*, 2006), Snf1 associates with 209 proteins, only 10% of which are enriched (hypergeometric test: $P=1.5E-5$) within *GO* carbohydrate metabolic process group (e.g., Adr1, Cat8, Sip4, Pho85, Gsy2, Reg1, Glc7). Moreover, similar to mammalian AMPK, Snf1 has been found to respond to various nutrient and environmental stresses including oxidative stress (Hong and Carlson, 2007), implicating a role for Snf1 as a global regulator in addition to controlling the usage of various carbon sources (Gancedo, 1998). Furthermore, the remarkable structural conservation of AMPKs' heterotrimeric complexes, specific

upstream activators, and downstream targets (at the transcriptional, protein synthesis and degradation, and posttranslational levels) in different kingdoms suggests a common AMPK ancestral function as a key regulator of energy homeostasis (Polge and Thomas, 2007).

Clarifying the organization and interactions of the Snf1 regulatory network is important for uncovering the complexity of global AMPK function and, ultimately, for using yeast as a model to study the role of AMPK in humans. However, neither transcriptional profiling, nor protein–protein interactions, nor ancestry alone can adequately describe the global regulatory role of Snf1. For this, a systems approach combining global measurements across different levels of the cellular hierarchy (mRNAs, proteins, and metabolites) is required. Recently, Ishii *et al* (2007) and Castrillo *et al* (2007) showed the utility of such an approach for mapping the cellular response of *Escherichia coli* and *Saccharomyces cerevisiae*, respectively, to genetic and environmental perturbations. Here, we integrated data from genome-wide mRNA and protein profiling and metabolite measurements with different networks comprising protein–protein interactions, protein–DNA interactions, and metabolic reaction stoichiometry, with the following objectives: (1) to show the use of novel algorithms for integrated analysis of high-throughput experimental datasets; (2) to reconstruct a global regulatory network for the protein kinase Snf1; and (3) to evaluate whether the components Snf1 and Snf4 of the Snf1 protein kinase complex have additional functions.

Results and discussion

Dataset collected in this study

We first collected a global dataset for wild-type *S. cerevisiae* CEN.PK113-7D and three Snf1 complex knockout mutants Δ*snf1*, Δ*snf4*, Δ*snf1*Δ*snf4* (Supplementary Table I) grown in triplicate in carbon-limited chemostat cultivations at a fixed dilution rate $D=0.100\,h^{-1}$ (see Materials and methods). Abundances of gene, protein, and intracellular metabolites were quantified using Affymetrix GeneChip Yeast Genome 2.0 Arrays (Wodicka *et al*, 1997), multidimensional protein identification technology (MudPIT) followed by quantitation using stable isotope labeling approach (Washburn *et al*, 2001; Usaite *et al*, 2008b), and gas chromatography coupled to mass spectrometry (Villas-Boas *et al*, 2005b), respectively. We quantified a total of 5667 transcripts, 2388 proteins, and 44 intracellular metabolites. At a threshold of $P<0.05$, a total of 1651, 1810, and 2395 mRNAs; 381, 396, and 352 proteins; and 20, 14, and 34 metabolites had significantly changed abundance levels in the knockout Δ*snf1*, Δ*snf4*, Δ*snf1*Δ*snf4* mutants compared with the wild-type strain, respectively (Supplementary Table II). However, only 159, 151, and 231 genes were identified to have significant changes in both mRNA and proteins in the knockout Δ*snf1*, Δ*snf4*, Δ*snf1*Δ*snf4* mutants compared with the wild-type strain, respectively. Among these there was the same change in abundance, that is both mRNA and protein were up- or downregulated, for 84, 87, and 88% of the proteins, respectively. Genes, whose mRNA and protein expression change correlated, belonged to carbon and amino-acid metabolism and indicated the presence of strong transcription regulation in these pathways. Genes, whose mRNA and protein had opposing significant expression changes, indicated dual level of regulation and, thus, the presence of physiologically meaningful regulation on protein level.

Integrated analysis for mapping Snf1 interactions

To show how the biological system was reprogramed as a result of deleting *SNF1*, *SNF4*, or both *SNF1* and *SNF4*, we applied four systems-wide methods that integrated our experimental measurements of mRNA, protein, and metabolites with data from protein–DNA binding (Hodges *et al*, 1999; Harbison *et al*, 2004), protein–protein interaction databases (Stark *et al*, 2006), and the yeast genome-scale metabolic model (Forster *et al*, 2003) (Figure 1). These four methods allowed us to identify reporter effectors reporter metabolites, high scoring sub-networks, and high scoring DNA-to-protein translation Onto a Graph-based Multi-level integrative Analysis (DOGMA) sub-networks, and based on this we reconstructed the global Snf1 kinase regulatory network (Figure 2). In total, our four different analyses identified the significant network interactions ($P<0.05$) in which the deletion of Snf1 has a critical function regulating global yeast metabolism (Figure 2E). As the metabolome dataset is relatively scarce we did not include this in our integrated data analysis, but only used these data to support some of our findings in terms of

Figure 1 A systems approach to mapping Snf1 response pathways. The panels depict the central dogma with highlights on the different levels of regulation captured by each method used in this work. Methods (**A**, **B**) are global methods to search for highly active biological sub-networks, whereas methods (**C**, **D**) are local scoring systems for evaluation of the regulatory significance, or 'activity', of effectors and metabolites. Each panel highlights the type of interaction/association that constitutes the basis of the underlying network graph used in the corresponding graph-based method. Nodes scored based on transcript level information are colored in gray. Nodes scored based on protein abundance information are colored in orange. Only nodes that are part of the interaction network are colored; for example, the transcript T2 is not colored in (C) as T2 is not part of the transcriptional regulatory network, but is colored in (B) because there is a translational association between T2 and P2. (A) Represents high scoring sub-network analysis (Ideker *et al*, 2001) that, based on gene expression data, was used to identify co-regulatory circuits of directly connected proteins and regulated genes that are significantly changing as a group in response to the loss of Snf1 kinase activity. (B) Represents a novel DOGMA sub-network approach (described here for the first time) that, based on gene and protein expression data, was used to identify co-regulatory circuits of directly connected proteins and regulated genes, and amplifies the significance of coordinated mRNA and protein expression that are significantly changing as a group in response to the loss of Snf1 kinase activity. (C) Represents Reporter Effector analysis tool (Oliveira *et al*, 2008) that, based on gene expression data, was used to identify TFs and regulatory proteins whose connected genes were most significantly affected and responded as a group to genetic disruptions of the Snf1 complex. Here, P1 is a TF that targets Gene 3, Gene 4, and Gene 5. (D) Represents Reporter Metabolite Analysis (Patil and Nielsen, 2005) that, based on gene (gray) or protein expression data (orange), was used for discovering metabolic hot spots that significantly responded to the loss of Snf1 kinase activity. (**E–H**) The number of component (mRNA or proteins) identified for the three different mutants in the different types of analysis.

how Snf1 is globally regulating metabolism. Below we describe the four different types of integrated analysis separately followed by a presentation of the metabolome data. Thereafter, we discuss how the results from the different types of analysis can be integrated into reconstruction of the global regulatory network.
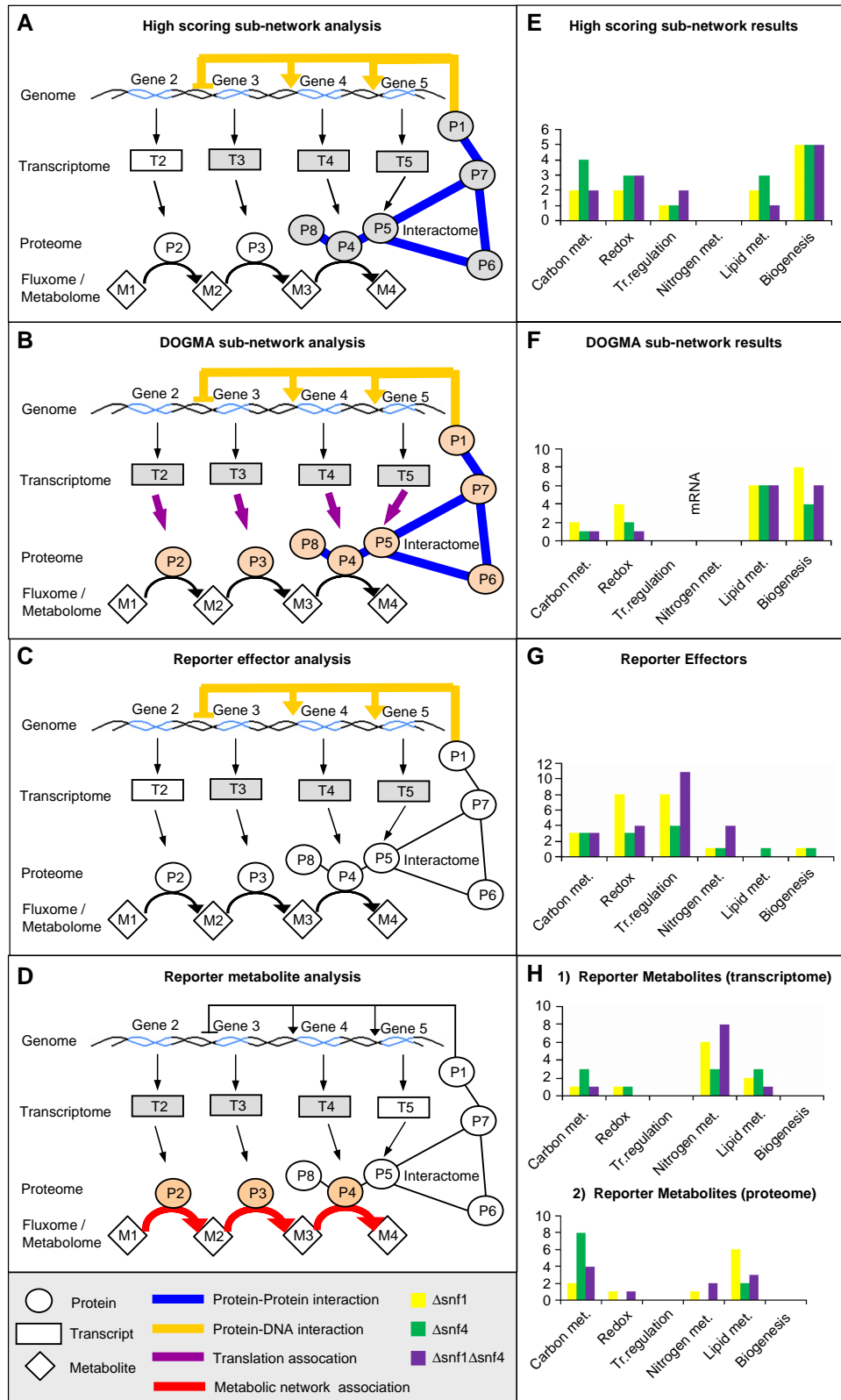
High scoring sub-network analysis

First, we used high scoring sub-network analysis (Ideker *et al*, 2002) to identify co-regulatory circuits of directly connected proteins and regulated genes that are significantly changing as a group in response to the loss of Snf1 kinase activity (Figure 1A) (see Materials and methods). We used high
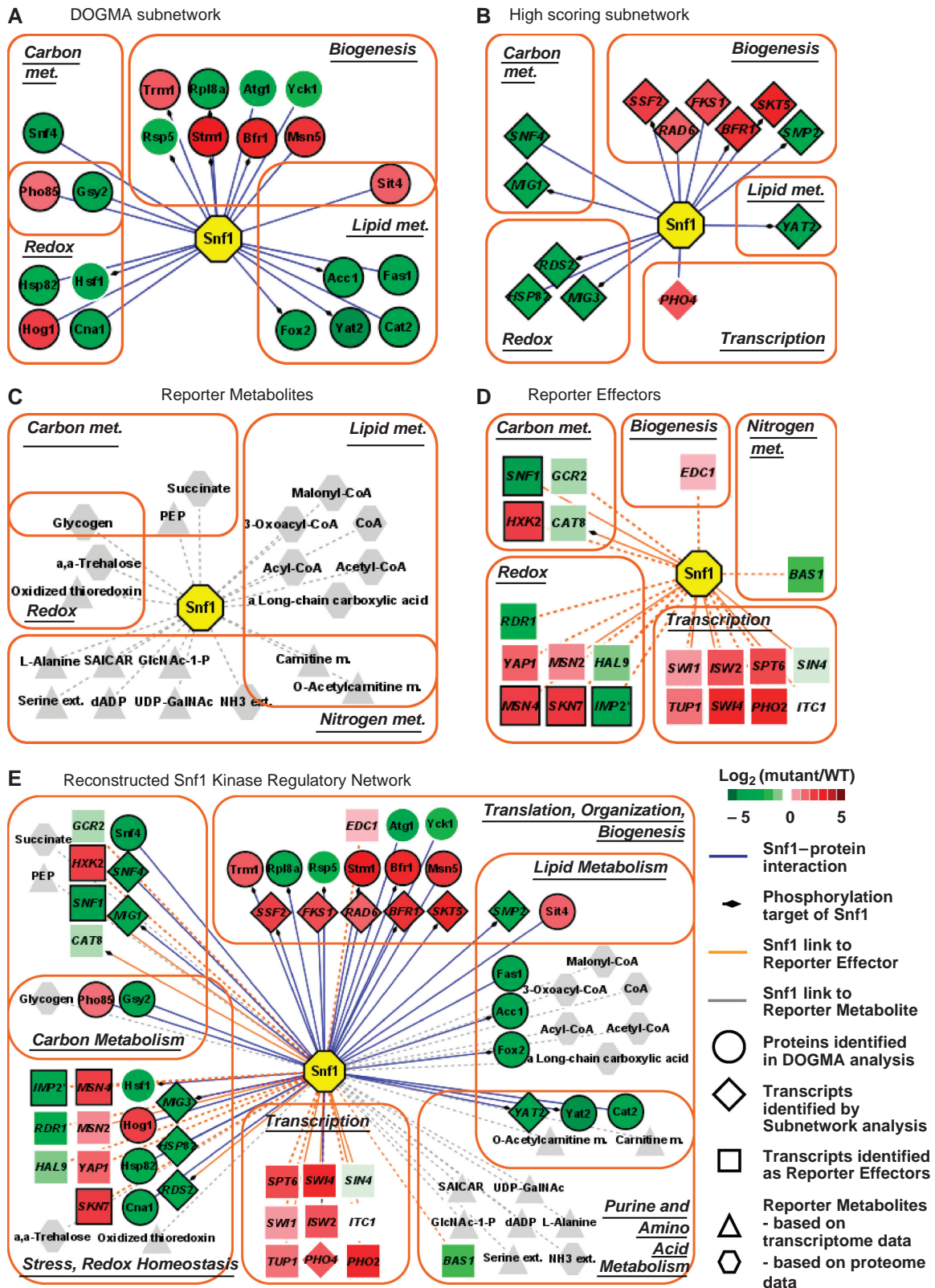
scoring sub-network analysis using mRNA data, as this is the only complete dataset covering expression of all genes in yeast and that potentially could accounts for all possible significantly changed protein and gene interactions. Not using protein expression data on protein nodes might skew high scoring sub-network analysis results in case of presence of posttranscription regulation, but still the analysis identifies transcriptionally co-regulated sub-networks. High scoring sub-network analysis showed three sub-networks comprising 301, 363, and 334 nodes and 651, 987, and 834 edges for the Δ*snf1*, Δ*snf4*, and Δ*snf1*Δ*snf4* mutants, respectively. From these co-regulated circuits, a total of 12, 18, and 13 proteins interacted with the Snf1 kinase (based on the definition of BIOGRID-Saccharomyces_cerevisiae v.2.0.25) for the Δ*snf1*, Δ*snf4*, and Δ*snf1*Δ*snf4* mutants, respectively. The results are summarized in Supplementary Table III and Figure 2B for the Δ*snf1* mutant. Only Snf1 kinase interacting proteins were included in the reconstructed Snf1 kinase regulatory network to represent the nodes most directly affected by the Snf1 kinase through protein interaction (Figure 2E). High scoring sub-network analysis identified expected glucose repression TF Mig1 as well as protein nodes in redox and biogenesis (Figure 2B). Results of the high scoring sub-network analysis were fairly consistent in terms of interactions with components of different parts of the metabolism for the three strains Δ*snf1*, Δ*snf4*, and Δ*snf1*Δ*snf4* (Figure 1E), but the targets vary somewhat between the strains (Supplementary Table III).

DOGMA sub-network analysis

To integrate our transcriptomics and proteomics measurements in the same analysis, we extended the high scoring sub-network analysis by mapping protein abundance data for protein nodes and mRNA data for DNA nodes, and included interaction edges between mRNA species and their corresponding proteins (Figure 1B). We call our new approach, which amplifies the significance of coordinated mRNA and protein expression, 'DOGMA sub-network analysis' (see Materials and methods). DOGMA sub-network analysis contains three types of interactions: protein–protein, protein—DNA, and 'mRNA to protein' translation interactions. The network expansion arises from the inclusion of interactions between each transcript (mRNA) and its corresponding protein. Changes in proteome levels were used to score protein

nodes, whereas transcriptome (mRNA) data were used to score DNA nodes. As for standard sub-network analysis, a simulated annealing algorithm was used to identify co-regulated regions in the network. DOGMA sub-network analysis identified three networks comprising 444, 450, and 376 nodes and 766, 740, and 609 edges for the Δ*snf1*, Δ*snf4*, Δ*snf1*Δ*snf4* mutants, respectively. Resulting high scoring sub-networks showed connected circuits being significantly regulated at gene, translation, and protein levels. From these co-regulated circuits, a total of 21, 14, and 16 proteins that interact with Snf1 kinase were identified for the Δ*snf1*, Δ*snf4*, Δ*snf1*Δ*snf4* mutants, respectively, and these are listed in Supplementary Table IV. Dogma sub-network analysis identified more Snf1 kinase interacting proteins involved in fatty acid and lipid metabolism compared with high scoring sub-network analysis results (Figure 2A and B) indicating the presence of significant posttranscriptional regulation in lipid metabolism. These results were consistent among the three strains studied (Figure 1F). Overall, both the high scoring sub-network and the DOGMA sub-network analysis identified a few proteins (e.g., Mig1, Snf4, Acc1, Gsy2) that were expected on the basis of earlier studies, but we also identified many other proteins interacting with Snf1, including proteins involved in carnitine metabolism (Yat2, Cat2), lipid metabolism (Smp2, Fas1, Fox2), and stress response (Hog1, Cna1). Strikingly, for all three strains studied, ∼85% of the first neighbors of the Snf1 kinase have a primary functional role outside the carbon metabolism including redox, lipid metabolism, and biogenesis.

Reporter effector analysis

We also applied our newly published 'Reporter Effector' algorithm (Oliveira *et al*, 2008) to identify TFs and regulatory proteins whose target genes were most significantly affected and responded as a group to genetic disruptions of the Snf1 complex (see Materials and methods and Figure 1C). Here, *Z*-scores for each effector were calculated based on the average of *Z*-scores of its adjacent genes (based on *P*-values from gene expression data) in a network of 3246 protein–DNA interactions and 484 effectors collected from ChIP-chip experiments and the YPD database (Hodges *et al*, 1999; Harbison *et al*, 2004). The cumulative *Z*-score was corrected for the size of the group and then converted back to *P*-values by using the normal

Figure 2 The reconstructed regulatory network of Snf1 kinase. The network was reconstructed by integrating mRNA and protein expression data for the Δ*snf1* mutant versus the wild-type strain with previously reported protein–DNA (Hodges *et al*, 1999; Harbison *et al*, 2004) and protein–protein (BIOGRID-Saccharomyces_cerevisiae v.2.0.25) (Stark *et al*, 2006) interactions, and with protein–metabolite interactions provided by the yeast genome-scale metabolic model (Forster *et al*, 2003). The network includes Snf1-interacting proteins that were identified by using gene expression data and high scoring sub-network analysis (blue connections to diamonds), or protein expression data and DOGMA analysis (blue connections to circles). Diamonds show gene expression data and circles show protein abundance data, which are colored according to log2-ratio color scale of Δ*snf1* relative to WT. The network also includes Reporter Metabolites, around which mRNA or protein abundance changes were significantly concentrated in response to the loss of *SNF1* (gray connections to triangles and hexagons, respectively). Reporter Effectors of Snf1 (orange connections to squares) show gene expression data. Reporter Effectors that are reported to associate to Snf1 kinase (Stark *et al*, 2006) are indicated using solid orange connections. Dashed lines indicate molecular or physiological links between Snf1 and the Reporter Effectors, or between Snf1 and the Reporter Metabolites not reported earlier. Small black arrow-diamonds represent previously determined Snf1-based phosphorylation of the Snf1 targets: Reporter Effectors and Snf1 interacting proteins (Ptacek *et al*, 2005). Nodes with black borders have significantly different (*P* < 0.05) mRNA or protein expression data for the Δ*snf1* mutant versus the wild-type strain. Genes and proteins are named according to the SGDatabase nomenclature. PEP, phosphoenolpyruvate; SAICAR, 1-(5′-phosphoribosyl)-5-amino-4-(*N*-succinocarboxamide)-imidazole; UDP-GalNAc, UDP-*N*-acetyl-D-galactosamine; GlcNAc-1-P, *N*-acetyl-D-glucosamine 1-phosphate; m, mitochondrial; ext, extracellular. More detailed information describing the sub-network, Reporter Effector, and Reporter Metabolite analyses outputs can be found in Supplementary Tables III–VII. (**A**) The components identified using the DOGMA sub-network analysis. (**B**) The components identified using the high scoring sub-network analysis. (**C**) The identified reporter metabolites. (**D**) The identified reporter effectors. (**E**) The combined and fully reconstructed interaction network for Snf1.

cumulative distribution function. The Reporter Effector analysis identified 22, 16, and 22 top-scoring ($P < 0.05$) effectors for the $\Delta snf1$, $\Delta snf4$, and $\Delta snf1 \Delta snf4$ mutants, respectively (Supplementary Table V; Figure 1G). Using Reporter Effector analysis, we identified significant transcription regulation hot spots within carbon, redox, global transcription regulation, and nitrogen metabolism. This analysis, for example, identified TFs that are known to be regulated by Snf1 kinase (i.e., Cat8), as well as TFs that are involved in redox, energy (Yap1, Skn7), nitrogen, and amino-acid (Bas1) metabolism and that have not previously been implicated as being regulated by Snf1 (Figure 2D; Supplementary Table V). Reporter Effector analysis identified that more transcription regulation changes are happening in the $\Delta snf1 \Delta snf4$ mutant compared with single deletion strains (Figure 1G). In particular, global regulatory factors, for example the TF Gcn4, of nitrogen and energy metabolism were identified only for the $\Delta snf1 \Delta snf4$ strain. This points to that in the double deletion strain there is stronger transcription regulation, in particular in term of regulation of the nitrogen metabolism.

Reporter metabolite analysis

Finally, we applied the Reporter Metabolite algorithm (Patil and Nielsen, 2005) to our gene and protein expression data for discovering metabolic hot spots that significantly responded to the loss of Snf1 kinase activity (see Materials and methods) (Figure 1D). Here, we queried a network comprising metabolic interactions derived from a genome-scale metabolic model consisting of 708 enzymes, 584 metabolites, and 1175 reactions (Forster *et al*, 2003). Each enzyme involved in this graph was then scored based on the significance of the change in the expression level of the corresponding gene or protein. The 10 top-scoring metabolites were identified as reporter metabolites. The reporter metabolites are those around which transcriptional (Supplementary Table VI) or protein expression (Supplementary Table VII) changes are significantly concentrated. Corroborating our analyses, the Reporter Metabolite approach identified key changes within carbon, energy (acetyl-CoA, succinate, glycogen, malonyl-CoA, long-chain carboxylic fatty acids), and redox metabolism (oxidized thioredoxin, NAD+/NADH) (Figure 2C), highlighting the significant Snf1 involvement in controlling energy homeostasis. There were differences in the identified reporter metabolites, when mRNA or protein datasets were subjected in the reporter metabolite analysis (Figure 1H-1 and H-2). For example, more reporter metabolites within nitrogen metabolic pathways were identified when mRNA was used compared with the use of proteome data. Thus, corroborating with the results of the Reporter Effector analysis, the reporter metabolite analysis indicated significant transcription regulation control within nitrogen metabolism (Figure 1H-1). More abundantly, reporter metabolites within carbon and lipid metabolism were identified only when protein dataset was used (Figure 1H-2), which supports results of the DOGMA sub-network analysis that indicates that the Snf1 kinase has a function in posttranscriptional control of fatty acid and lipid metabolism.

Metabolome profiling

Forty-four intracellular metabolites were quantified in the four strains of the study. As collected metabolome dataset was limited compared with complete yeast cell metabolome profiling, our metabolome dataset was only used to support the integrated data analysis. The collected metabolome dataset is given in Supplementary Table VIII. The metabolome dataset correlated well with the Reporter Metabolite analysis results, for example indicating significant changes in amino acid and energy (NAD+/NADH) metabolism for the double deletion strain, and indicating significant changes in mostly carbon and lipid metabolism for the $\Delta snf4$ strain.

Differences and similarities of strains $\Delta snf1$, $\Delta snf4$, and $\Delta snf1 \Delta snf4$

This study is the first, in which the $\Delta snf1$, $\Delta snf4$, and $\Delta snf1 \Delta snf4$ strains were studied in parallel using several high-throughput analytical techniques. The larger number of significant changes identified on the transcriptome and metabolome levels indicated that the double deletion strain is different compared with the single deletion strains (Supplementary Table 1). The double deletion strain was also shown to have a different phenotype with respect to growth on galactose (Usaite *et al*, 2008a) and it was also found earlier to have a larger change in the proteome compared with the single deletion strains (Usaite *et al*, 2008b). In this study, our four data integration and analysis tools identified and demonstrated strain-specific differences. Even though, the reconstructed Snf1 regulatory networks seemed to be quite similar, when derived based on the data for each of the $\Delta snf1$, $\Delta snf4$, and $\Delta snf1 \Delta snf4$ strains (Figure 2E; Supplementary Figures 1 and 2), some regulatory differences can be identified. The Reporter Effector and Reporter Metabolite analysis identified the most crucial differences among the three strains studied (Figure 1G, H-1, and H-2). Reporter Metabolite analysis indicated that deleting *SNF4* gene affected mainly only carbon metabolism (Figure 1H-1 and H-2). Unexpectedly, deletion of both *SNF1* and *SNF4* genes induced changes in transcription regulation and in particular in nitrogen metabolism (Figure 1G, H-1, and H-2). Overall, our data integration analysis showed that the $\Delta snf1$ and $\Delta snf4$ strains are being more alike whereas the double deletion $\Delta snf1 \Delta snf4$ strain is behaving differently. Our results indicated that deletion of both *SNF1* and *SNF4* genes cause a synergistic effect that is caused changes in transcription regulation mechanisms and in particular abundant changes in the regulation of nitrogen metabolism (Figure 1G, H-1, and H-2). Our three-level ome-data analysis approach demonstrated to be a good tool to successfully characterize all strains of the study and identify strain-specific differences.

Snf1 regulates carbon metabolism—validity of our systems approach analysis

At the core of the Snf1 regulatory network (Figure 2E), there are players known to be affected by Snf1, for example components of the glucose repression system: Mig1, Hxk2, and Cat8. For example, Cat8 regulates the glyoxylate cycle by

controlling expression of the *ICL1*, *MLS1*, and *MDH2* genes (Schuller, 2003). Consistent with the importance of the Snf1–Cat8 interaction, the expression of these metabolic genes, their coding proteins, and the measured level of intracellular glyoxylate were significantly lower in the Δ*snf1* mutant relatively to the wild-type strain ($P<0.05$) (Supplementary Figure 3; Supplementary Tables VIII and IX) (and the double deletion mutant). Overall, the results showed a high degree of correlation for glucose repression related genes, their coding proteins, and pathway metabolites (Supplementary Figure 3). Our results correlates with prior knowledge of glucose repression regulatory cascade studies (Gancedo, 1998; Schuller, 2003) and reemphasize that transcriptional regulation is the primary glucose repression control mechanism. These results also validate our approach.

Corroborating with previous knowledge, our analysis also identified that Snf1 kinase regulates energy storing pathways. First, glycogen was identified as reporter metabolite (Figure 2C; Supplementary Table VII) in Reporter Metabolite analysis based on protein expression data. Glycogen synthase, Gsy2, and its activity regulating Pho85 (Hardy *et al*, 1994) were identified in DOGMA sub-network analysis as being some of the most significantly changed network players affected by the loss of Snf1 kinase activity (Figure 2E). Snf1 control of Msn2,4, which regulates the expression of *GSY1* encoding glycogen synthase (Hardy *et al*, 1994; Unnikrishnan *et al*, 2003), was also implicated (Figure 2E; Supplementary Table IX). Overall, our three-level ome-data integrated analysis results showed that energy storing pathways are down-regulated through an Snf1-dependent mechanism.

Snf1 is shown as a low-energy checkpoint

Mammalian AMPK is described as a low-energy checkpoint that mediates the energy state of the cell by regulating catabolic and anabolic reactions, that is inducing energy generating and repressing energy consuming reactions under low energy (Hardie and Sakamoto, 2006). Recent reviews have also implied that the yeast Snf1 protein kinase is a global energy regulator (Polge and Thomas, 2007; Hardie, 2007b). However, global evidence across multiple levels of the cellular hierarchy has still been lacking. Our three-level ome-data and systems-wide data analysis for the first time support this hypothesis and demonstrates yeast Snf1 kinase being a global energy regulator. A particular strength of our analysis is that we compared the strains at carbon-limited growth conditions in which the Snf1 protein kinase is supposed to be active, whereas most other studies have used shake flasks where there is normally carbon excess and the role of Snf1 protein kinase is therefore relatively small.

Snf1 kinase regulates β-oxidation on protein level

High scoring sub-network analysis identified the most significant factors associated with Snf1 to be Fox2, Acc1, and Fas1 (Figure 2A and B). To explore how these pathways were affected, we built a pathway model linking identified significant changes across all measurement types (transcriptome, metabolome, proteome) in Cytoscape (Shannon *et al*, 2003) (Figure 3). Using this model, it was possible for us to

identify a relatively complex regulatory system around lipid metabolism. Genes and proteins (Cta1, Pox1, Fox2, and Pot1) involved in β-oxidation had significantly ($P<0.05$) lower expression in the three Snf1 kinase complex mutants relative to the wild type. In agreement, quantitative metabolome analysis showed that free fatty acids (oleic, palmitoleic, myristic, palmitic, and stearic acid) accumulated in the Snf1 kinase complex mutants relatively to the wild-type strain, rather than being catabolized by β-oxidation to generate energy (Supplementary Table VIII). Thus, it is quite clear that loss of Snf1 kinase complex activity leads to a decreased activity in energy producing pathways such as β-oxidation. Furthermore, our DOGMA and Reporter Metabolite analysis, demonstrate that Snf1 kinase regulates fatty acid metabolism through far more complex, that is using both protein–protein interaction and regulation of carnitine metabolism, rather than only through transcriptional regulation of β-oxidation as reported earlier (Young *et al*, 2002; Schuller, 2003).

Yeast Snf1 kinase controls carnitine transfer system

Our systems approach analysis clearly demonstrated that the carnitine transfer system in yeast are under the control of the Snf1 kinase complex, even though no prior references describing Snf1 control of this system have been reported for yeast. First, it was found that Snf1 kinase interacts with the carnitine transferase proteins Cat2 and Yat2 through the sub-network analyses (both proteins were shown to have lower protein and gene expression levels when the Snf1 kinase complex was disrupted, Figures 2A and 3). Second, malonyl-CoA and carnitine derivatives were identified as reporter metabolites (indicating that significant changes in gene and protein expression are centered around these metabolites) (Figure 2C). It is found that the carnitine metabolic and transfer system has a rate-limiting function in fatty acid β-oxidation in humans and it is regulated by AMPK through controlling the level of malonyl-CoA (Folmes and Lopaschuk, 2007). In yeast, β-oxidation is cytosolic, but still transport of fatty acids across the mitochondrial membrane may have a role in overall lipid metabolism and Snf1-associated regulation at this level may therefore have an even wider role on global regulation of lipid metabolism in yeast.

Snf1 kinase in control of fatty acid and lipid biosynthesis

The DOGMA sub-network analysis identified lower expression of *de novo* lipid biosynthesis involving Acc1, Fas1 (and Smp2), when the Snf1 protein kinase complex mutants were compared to wild-type cells (Supplementary Table IV; Figure 2A). In addition, the metabolome analysis identified increased levels of free fatty acids, serine, and glycine in the Snf1 protein kinase mutants (Supplementary Table VIII; Figure 3). Consistently with earlier results (Grauslund *et al*, 1999; Young *et al*, 2002), the expression of *GUT1* coding for protein catalyzing the formation of glycerol-3-phosphate (the structural backbone of many lipids) was decreased, when Snf1 kinase complex was inactivated in the Δ*snf1*, Δ*snf4*, and
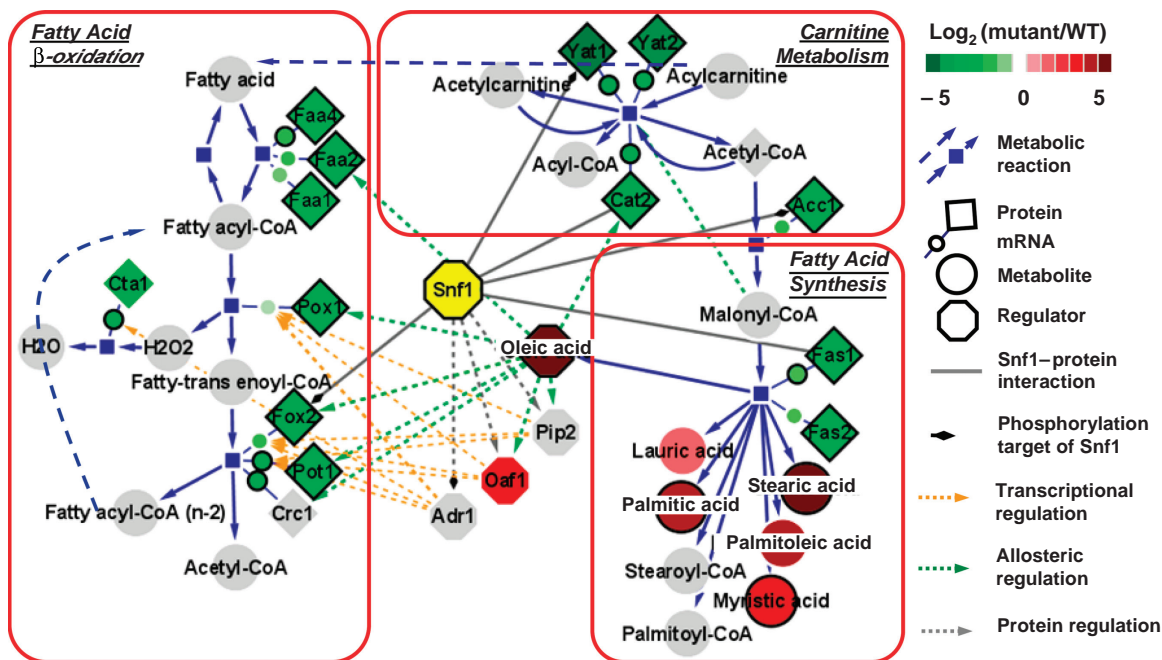
Figure 3 The impact of Snf1 kinase on fatty acid metabolism shows its role as a global energy regulator. This figure comprises information of the yeast metabolic network (Forster *et al*, 2003), the reconstructed Snf1 regulatory network, and raw mRNA, protein and metabolite abundance data for the Δ*snf1* mutant compared with the wild-type strain (Figure 2; Supplementary Tables VIII and IX). This figure shows that the loss of Snf1 activity results in reduced activity of energy producing reactions (e.g., β-oxidation). Enzymes are mapped using protein (in diamonds) and mRNA (in small circles) expression data, which is colored according to log2-ratio color scale. Available protein and metabolite relative abundance data are mapped on the regulators and metabolites, accordingly. Nodes with black borders have significantly different ($P < 0.05$) expression data for the Δ*snf1* mutant versus the wild-type strain. Gray nodes represent components that were not measured. Five Snf1–protein interactions (solid gray lines) were identified using sub-network analyses. Colored dashed lines indicate previously reported protein, transcriptional, and allosteric regulations (Young *et al*, 2002; Schuller, 2003).

Δ*snf1*Δ*snf4* mutants (Figure 3; Supplementary Table IX). Intuitively it could be misleading that there is an increased level of the free fatty acids when there is transcriptional downregulation of the biosynthetic genes, but our integrated analysis allows a more global insight into the regulation of fatty acid biosynthesis (see above discussion on downregulation of β-oxidation). In this context it is interesting to mention that the Snf1 protein kinase is known to inactive acetyl-CoA carboxylase, a key enzyme catalyzing the entry into lipid metabolism, and clearly there can be no inactivation of this enzyme in the deletion strains. This could mean that despite downregulation of Acc1 the fraction of the present enzyme that is active may be higher in the deletion strains, which is further supported by the fact that the phosphate Sit4, which activates Acc1, is found to be more abundant in both the Δ*snf1* (Figure 2E) and Δ*snf4* (Supplementary Figure 1) strains. This points to a quite complex regulation around the entry into lipid metabolism, and solid conclusions on this regulatory node would require a far more in-depth analysis of this node involving detailed lipid analysis. However, the accumulation of precursors for phospholipid biosynthesis points to a downregulation of lipid metabolism, or at least loss of coordinated regulation of this very complex biosynthesis.

As experiments were performed in carbon (energy)-limited growth conditions, lower energy production through β-oxidation, as a consequence of the inactivation of Snf1 kinase complex, should affect energy consumption in the cell. Substantiating this hypothesis, we found that there was

repression of energy consuming (e.g., fatty acid and lipid biosynthesis) pathways in the mutants relative to the wild-type strain (Figure 3; Supplementary Figure 3), and the net effect is likely that there was a decreased flux into lipid biosynthesis in the Snf1 protein kinase deleted strains.

Snf1 as a regulator of redox metabolism

Interestingly the *GO* molecular function category *Oxidoreductase Activity* was enriched (hypergeometric test: $P = 5E-07$ and $6E-03$) for both mRNA and proteins whose abundance was found to be significantly changed. The systems analysis also implicated multiple genes, proteins, and metabolites that respond to redox change or are involved in redox maintenance (Yap1, Skn7, Msn2,4, Bas1, Pho2, Ssa1, Hsf1, Gts1, Fas1, Fox2, oxidized thioredoxin, NAD$^+$/NADH, glutathione) (Figure 2; Supplementary Tables III–VII). On the basis of an earlier observed Yap1–Sip2 protein interaction (Wiatrowski and Carlson, 2003), we suggested that the Snf1 protein kinase (in complex with Sip2) may contribute to controlling redox homeostasis directly through the TF Yap1 rather than through global regulation of respiration and fluxes through key catabolic pathways. Specifically, the significantly lower expression was found among genes (e.g., *CTT1*, *SOD1*, *SOD2*, *GPX2*) that are involved in maintaining the redox balance and are regulated by oxidative stress through Yap1 (Supplementary Table IX). The data indicate that a lower oxidative stress, thus, a less-induced oxidative stress defense

system, is present in the mutants versus the wild type in this study. This could be linked to the reduced oxidative activity in the mutant strains as a consequence of the downregulation of β-oxidation (Canto *et al*, 2009). Thus, again we conclude that even though Snf1 has a key function in regulating lipid metabolism, it needs also to regulate other parts of the metabolism as alteration in lipid metabolism requires adjustment in many other parts of the metabolism to ensure metabolic homeostasis.

Summary

Collectively, our systems approach identified that energy generating β-oxidation pathways, energy consuming fatty acid synthesis, and energy storing and homeostasis pathways were significantly affected by the loss of Snf1 kinase activity during carbon-limited growth. This represents the first systems-wide analysis using three types of high-throughput data for mapping the integrated nature and control that the Snf1 protein kinase has in regulating these pathways. Our results clearly show that Snf1 is mimicking the role of its orthologue AMPK in mammalian cells as a low-energy checkpoint. Interestingly, our analysis shows that Snf1 interacts with many pathways that may also be linked to the protein kinase Tor1 (for example, amino acid, energy and lipid metabolic pathways), and thus our results suggest that Snf1 and Tor1 both have a role in integrating information on the nutritional state and in concert control energy and redox metabolism. Interestingly, our data point to that the two components of the Snf1 protein kinase complex Snf1 and Snf4 may interact with other proteins and hereby exert additional functions. However, these functions are quite consistent with the global role of the Snf1 protein kinase, and we therefore speculate that without deleting both the Snf1 and Snf4 sub-units there is not a full inactivation of the protein complex.

We have combined global data measurements from three levels of the cell (mRNAs, proteins, and metabolites) to construct a regulatory map of Snf1 kinase. The regulatory map reconstructed here identified new Snf1 targets and confirmed previously described connections, validating the power of our systems approach. Our analysis showed that Snf1 kinase regulates multiple cellular pathways overall acting as a low-energy checkpoint. Using our systems approach, novel Snf1 targets and their regulation on gene or protein level (in response to the loss of active Snf1) were identified. The yeast carnitine metabolic and transfer system was shown to be controlled by the Snf1 kinase. Highlighting the importance of measuring both mRNAs and proteins, Snf1 neighbors identified only in DOGMA sub-network analysis implied important posttranscriptional regulation effects. For example, by only identifying Acc1 in DOGMA analysis, our results indicate that Acc1, which is phosphorylated and inactivated by Snf1 (Shirra *et al*, 2001), is regulated on the protein synthesis and degradation level by the Snf1 kinase complex. As Pho85 and Gsy2 were also only identified as Snf1 first neighbors in DOGMA sub-network analysis, combined gene expression and protein level data indicate that posttranscriptional control through Pho85 and Gsy2 regulates glycogen metabolism when Snf1 kinase is inactive. Owing to the mode of action of Snf1 kinase activity, measuring both gene expression and protein

levels is an appropriate strategy for identifying regulatory structure. Intracellular metabolome data were further used to validate changes in metabolic pathways, which through our network analysis were identified to be Snf1 controlled (e.g., glyoxylate as described above) (Figure 3; Supplementary Figure 3). Measured free fatty acids (Supplementary Table VIII) highlighted the importance of available metabolome data and contributed to our understanding of role of Snf1 in controlling lipid metabolism and energy homeostasis. Overall, our results indicate the beneficial contribution of using measurements from multiple cellular levels to reconstruct regulatory networks. Our work strengthens the homology in function between yeast Snf1 and mammalian AMPK and opens the door for further using yeast as a model organism to study AMPK and hereby use our reconstructed network as a scaffold for better understanding and ultimately address metabolic disorders in humans.

Materials and methods

Strains and cultivation

The *S. cerevisiae* strains used in this study were a prototrophic strain CEN.PK 113-7D (*MAT*a *MAL2-8*c *SUC2*) (Van Dijken *et al*, 2000), its derivatives Δ*snf1* and Δ*snf4* supplied by Koetter (Frankfurt, Germany) and Δ*snf1*Δ*snf4* generated by Usaite *et al* (2008a). The only genotypic difference among strains used is summarized in Supplementary Table I. Steady-state aerobic chemostat cultures were grown at 30°C in 2 l bioreactors (Braun B) using a dilution rate of $D=0.100$ (± 0.005) h^{-1}. Chemostat cultivation ensured that metabolic and regulatory changes observed were specific to disruptions of the Snf1 complex, and not complicated by external effects resulting from the specific mutant physiology (e.g., different growth rates). Detailed description of the cultivations performed and the composition of the carbon-limited minimal medium used was summarized earlier (Usaite *et al*, 2008b). After steady state was reached, the cell samples for metabolome, transcriptome, and proteome analyses were collected.

Transcriptome data acquisition

Samples for RNA isolation were taken from chemostat cultivations as described earlier (Usaite *et al*, 2006). Total RNA was extracted by using a FastRNA Pro Red kit (BIO 101 Systems, Inc, Vista, CA). The cDNA synthesis, cRNA synthesis, labeling, and cRNA hybridization on the oligonucleotide array Yeast_2.0 (Affymetrix, CA) were performed as described in the Affymetrix GeneChip expression analysis manual that was downloaded from the Affymetrix website in October 2004. The Yeast_2.0 arrays were scanned with the GeneChip 3000 7G Scanner. The Affymetrix microarray suite v5.0 was used to generate CEL image files of the arrays. The array images were then normalized and the transcript levels of all *S. cerevisiae* probe sets were calculated with the perfect-match model in dChip v1.2 (Li and Wong, 2001). The gene expression data are available on the ArrayExpress. The accession number is E-MEXP-1407.

Proteome data acquisition

Quantitative proteome data were generated and described by us earlier (Usaite *et al*, 2008b). Briefly, samples for total protein were collected from chemostat cultivations, cells were lysed, and total protein was extracted. Protein concentration per sample was determined, and ^{14}N-labeled and ^{15}N-labeled samples were mixed 1:1 by protein weight. A total of 200 μg of total protein was chemically modified and digested by trypsin and endoproteinase LysC. The protein pool digest was analyzed using MudPIT (Washburn *et al*, 2001). A tandem mass spectrum was analyzed and relative protein abundance was quantified using stable isotope labeling as described earlier (Venable *et al*, 2007;

Usaite *et al*, 2008b). Complete list of proteins, for which abundances were found to be significantly ($P<0.05$) changed (in the Δ*snf1*, Δ*snf4*, and Δ*snf1*Δ*snf4* versus wild-type strain), based on the stable isotope labeling approach is available at http://pubs.acs.org as Supplementary information to Usaite *et al* (2008b).

Metabolome data acquisition

Cells from chemostat cultivations were rapidly quenched according to de Koning and van Dam (1992). Cells were centrifuged at 10 000 *g* for 3 min in −20°C to separate the cells from the quenching solution. Chloroform: methanol: buffer extraction and pure methanol extraction (MEOH) were carried out (Villas-Boas *et al*, 2005a). Samples were freeze dried at −56°C using a Christ-Alpha 1–4 freeze dryer (Villas-Boas *et al*, 2005b). Amino and non-amino organic acid levels were determined by GC-MS analysis according to Villas-Boas *et al* (2005b) except that a Finnegan FOCUS gas chromatograph coupled to single quadrupole mass selective detector (EI) (Thermo Electron Corporation, Waltham, MA, USA) was used. Peak enumeration was conducted with AMDIS (NIST, Gaithersburg, MD) with default parameters, and identification of conserved metabolites was conducted with Spect-Connect (Styczynski *et al*, 2007), using default parameters and a support threshold of 3. As SpectConnect is unable to resolve metabolite peaks that have similar MS spectra and are close in time, hand curation of the AMDIS output files was also performed. Samples were normalized by an internal standard chlorophenylalanine (30 µl of a 4 mM solution was added before extraction) and by the biomass weight per sample. The identified and quantified metabolites are listed in Supplementary Table VIII.

Reporter metabolite analysis

To identify metabolic hot spots that significantly responded to the Snf1 kinase complex disruption at the gene or protein expression level (Patil and Nielsen, 2005), gene or protein expression changes in response to *SNF1* or *SNF4* gene deletion were mapped on the genome-scale metabolic model of *S. cerevisiae* (Forster *et al*, 2003). The genome-scale model of yeast was first represented as a graph in which each metabolite is connected to all enzymes that catalyze a reaction involving that particular metabolite. Each enzyme involved in this graph was then scored based on the significance of change in the expression level of the corresponding gene or protein. This significance score was calculated by using a *t*-test and the resulting *P*-value was transformed to a *Z*-score using the inverse normal cumulative distribution function. Each metabolite was assigned the average score of its *k* neighboring enzymes, and this score was then corrected for the background by subtracting the mean and dividing by the standard deviation of average scores of 10 000 enzyme groups of size *k* selected from the same dataset. These corrected scores were then converted back to *P*-values by using the normal cumulative distribution function. The 10 top-scoring metabolites were identified as reporter metabolites and selected for the analysis in this study. Thus, the reporter metabolites are those around which transcriptional (Supplementary Table VI) or protein expression (Supplementary Table VII) changes are significantly concentrated.

Reporter effector analysis

The Reporter Effector algorithm is an integrative method that combines the topology of the regulatory network (effector—gene) with gene expression levels, to identify those effectors (TFs, other regulatory proteins) whose connected genes are most significantly responsive as a group to a perturbation (Oliveira *et al*, 2008). Gene expression for a total of 484 effectors and their 968 targets, and 3246 protein–DNA interactions collected from ChIP-chip experiments (Hodges *et al*, 1999; Harbison *et al*, 2004) were used to perform the Reporter Effector analysis. Each effector was scored based on the average of scores of its adjacent genes (corrected for the size of the group of connected genes), and the high scoring effectors are termed Reporter Effectors. Reporter Effectors highlight the regulatory pathways affected following a perturbation, and thus uncover the functional links between the perturbation and the consequent regulatory mechanisms invoked in the cell. Many TFs and regulators do not respond at transcriptional level *per se* (but through posttranslational regulation instead): Reporter Effector analysis therefore provides a powerful tool for reconstruction of regulatory circuits without *a priori* requirement of change in the transcription level of the regulators. In this study, the Reporter Effector analysis was performed three times (first using the complete gene expression dataset, second using only genes with reduced expression, and third using only genes with increased expression, having gene expression datasets for any two-strain comparison) to account for repressing, activating, or dual role having TFs. The top-scoring reporter effectors ($P<0.05$) were selected (Supplementary Table V) for the analysis in this study.

Sub-network analysis

To search for the high scoring sub-networks that describe highly active regulatory modules of connected proteins and regulated genes that are significantly changing in response to a perturbation, we used the previously proposed simulated annealing algorithm (Ideker *et al*, 2002) implemented with an additional heuristics: the probability of a certain node being marked visible in the initialization was proportional to $(1-P\text{-value})$. Briefly, the algorithm takes as inputs a graph *G* (i.e., one of the interaction networks) and a list of *P*-values (in this case, from a two-tail Student's *t*-test, reflecting the changes in transcript/protein levels between each mutant and the reference strain). *P*-values are converted into *z*-scores using the inverse cumulative distribution function. *Z*-scores are then mapped into the graph, and the score of a given sub-network *SG* is calculated as the average sum of all node elements of *SG*, corrected for background and for the size of *SG*. To find the highest score sub-network, a simulated annealing algorithm is used. As referred by Ideker *et al*, and because the problem of finding the highest score connected sub-network is NP-hard, it is not guaranteed to find the overall maximum using this algorithm (Ideker *et al*, 2002; *Bioinformatics*). Therefore, each pair of network/data was analyzed 10 times, and we use the results obtained from merging the 10 high scoring sub-networks.

Here, a large network comprising 57 680 protein–protein interactions and 10 884 protein–DNA interactions was used for this analysis. From the BioGRID database (BIOGRID-Saccharomyces_cerevisiae v.2.0.25), a downloaded list of protein–protein interactions was curated by removing duplicated information and by selecting protein physical interactions generated using Affinity Capture-MS, Affinity Capture-RNA, Affinity Capture-Western, Biochemical Activity, Co-crystal Structure, Co-fractionation, Co-localization, Co-purification, FRET, Far Western, Protein-RNA, Protein-peptide, Reconstituted Complex, and Two-hybrid methods. This resulted in obtaining 57 680 protein–protein interactions, covering 3868 unique proteins. A total of 10 884 high-confidence (P-value <0.001) protein–DNA interactions derived from ChIP-chip data (Harbison *et al*, 2004) were included in high scoring sub-network analysis.

DOGMA sub-network analysis

This analysis contained three types of interactions: protein–protein, protein—DNA, and 'mRNA to protein' translation interactions. As we quantified both mRNA and protein abundances, the network of biomolecular interactions was extended to accommodate both changes in transcript and protein levels. Namely, we had a chance to expand network analysis including the translational relationship between each transcript *i* and the corresponding protein *i*. Changes in proteome levels were used to score protein nodes, whereas transcriptome data were used to score gene nodes. Therefore, the resulting high scoring DOGMA sub-networks showed connected circuits being significantly regulated at gene, translation and protein levels. First Snf1 kinase neighbors (Snf1-interacting proteins) that were identified using DOGMA sub-network (Supplementary Table IV) were subjected in more detail analysis of this study.

Supplementary information

Acknowledgements

Conflict of interest

The authors declare that they have no conflict of interest.

References

Canto C, Gerhart-Hines Z, Feige JN, Lagouge M, Noriega L, Milne JC, Elliott PJ, Puigserver P, Auwerx J (2009) AMPK regulates energy expenditure by modulating NAD + metabolism and SIRT1 activity. *Nature* **458:** 1056–1060

Carlson M (1999) Glucose repression in yeast. *Curr Opin Microbiol* **2:** 202–207

Castrillo JI, Zeef LA, Hoyle DC, Zhang N, Hayes A, Gardner DC, Cornell MJ, Petty J, Hakes L, Wardleworth L, Rash B, Brown M, Dunn WB, Broadhurst D, O'donoghue K, Hester SS, Dunkley TP, Hart SR, Swainston N, Li P *et al* (2007) Growth control of the eukaryote cell: a systems biology study in yeast. *J Biol* **6:** 4

Celenza JL, Carlson M (1986) A yeast gene that is essential for release from glucose repression encodes a protein kinase. *Science* **233:** 1175–1180

de Koning W, van Dam K (1992) A method for the determination of changes of glycolytic metabolites in yeast on a subsecond time scale using extraction at neutral pH. *Anal Biochem* **204:** 118–123

DeRisi JL, Iyer VR, Brown PO (1997) Exploring the metabolic and genetic control of gene expression on a genomic scale. *Science* **278:** 680–686

Folmes CDL, Lopaschuk GD (2007) Role of malonyl-CoA in heart disease and the hypothalamic control of obesity. *Cardiovasc Res* **73:** 278–287

Forster J, Famili I, Fu P, Palsson BO, Nielsen J (2003) Genome-scale reconstruction of the *Saccharomyces cerevisiae* metabolic network. *Genome Res* **13:** 244–253

Gancedo JM (1998) Yeast carbon catabolite repression. *Microbiol Mol Biol Rev* **62:** 334–361

Grauslund M, Lopes JM, Ronnow B (1999) Expression of *GUT1*, which encodes glycerol kinase in *Saccharomyces cerevisiae*, is controlled by the positive regulators Adr1p, Ino2p and Ino4p and the negative regulator Opi1p in a carbon source-dependent fashion. *Nucleic Acids Res* **27:** 4391–4398

Harbison CT, Gordon DB, Lee TI, Rinaldi NJ, Macisaac KD, Danford TW, Hannett NM, Tagne JB, Reynolds DB, Yoo J, Jennings EG, Zeitlinger J, Pokholok DK, Kellis M, Rolfe PA, Takusagawa KT, Lander ES, Gifford DK, Fraenkel E, Young RA (2004) Transcriptional regulatory code of a eukaryotic genome. *Nature* **431:** 99–104

Hardie DG (2007a) AMP-activated protein kinase as a drug target. *Ann Rev Pharmacol Toxicol* **47:** 185–210

Hardie DG (2007b) AMP-activated/SNF1 protein kinases: conserved guardians of cellular energy. *Nat Rev Mol Cell Biol* **8:** 774–785

Hardie DG, Sakamoto K (2006) AMPK: a key sensor of fuel and energy status in skeletal muscle. *Physiology* **21:** 48–60

Hardy TA, Huang D, Roach PJ (1994) Interactions between cAMP-dependent and SNF1 protein kinases in the control of glycogen accumulation in *Saccharomyces cerevisiae*. *J Biol Chem* **269:** 27907–27913

Hodges PE, McKee AH, Davis BP, Payne WE, Garrels JI (1999) The Yeast Proteome Database (YPD): a model for the organization and presentation of genome-wide functional data. *Nucleic Acids Res* **27:** 69–73

Hong SP, Carlson M (2007) Regulation of snf1 protein kinase in response to environmental stress. *J Biol Chem* **282:** 16838–16845

Ideker T, Ozier O, Schwikowski B, Siegel AF (2002) Discovering regulatory and signalling circuits in molecular interaction networks. *Bioinformatics* **18**(Suppl 1): S233–S240

Ideker T, Thorsson V, Ranish JA, Christmas R, Buhler J, Eng JK, Bumgarner R, Goodlett DR, Aebersold R, Hood L (2001) Integrated genomic and proteomic analyses of a systematically perturbed metabolic network. *Science* **292:** 929–934

Ishii N, Nakahigashi K, Baba T, Robert M, Soga T, Kanai A, Hirasawa T, Naba M, Hirai K, Hoque A, Ho PY, Kakazu Y, Sugawara K, Igarashi S, Harada S, Masuda T, Sugiyama N, Togashi T, Hasegawa M, Takai Y *et al* (2007) Multiple high-throughput analyses monitor the response of *E. coli* to Perturbations. *Science* **316:** 593–597

Kahn BB, Alquier T, Carling D, Hardie DG (2005) AMP-activated protein kinase: ancient energy gauge provides clues to modern understanding of metabolism. *Cell Metab* **1:** 15–25

Li C, Wong WH (2001) Model-based analysis of oligonucleotide arrays: expression index computation and outlier detection. *Proc Natl Acad Sci USA* **98:** 31–36

Oliveira AP, Patil KR, Nielsen J (2008) Architecture of transcriptional regulatory circuits is knitted over the topology of bio-molecular interaction networks. *BMC Syst Biol* **2:** 17

Patil KR, Nielsen J (2005) Uncovering transcriptional regulation of metabolism by using metabolic network topology. *Proc Natl Acad Sci USA* **102:** 2685–2689

Polge C, Thomas M (2007) SNF1/AMPK/SnRK1 kinases, global regulators at the heart of energy control? *Trends Plant Sci* **12:** 20–28

Ptacek J, Devgan G, Michaud G, Zhu H, Zhu X, Fasolo J, Guo H, Jona G, Breitkreutz A, Sopko R, McCartney RR, Schmidt MS, Rachidi N, Lee SJ, Mah AS, Meng L, Stark MJ, Stern DF, De Virgilio C, Tyers M *et al* (2005) Global analysis of protein phosphorylation in yeast. *Nature* **438:** 679–684

Schuller HJ (2003) Transcriptional control of nonfermentative metabolism in the yeast *Saccharomyces cerevisiae*. *Curr Genet* **43:** 139–160

Shannon P, Markiel A, Ozier O, Baliga NS, Wang JT, Ramage D, Amin N, Schwikowski B, Ideker T (2003) Cytoscape: a software environment for integrated models of biomolecular interaction networks. *Genome Res* **13:** 2498–2504

Shirra MK, Patton-Vogt J, Ulrich A, Liuta-Tehlivets O, Kohlwein SD, Henry SA, Arndt KM (2001) Inhibition of acetyl coenzyme A carboxylase activity restores expression of the *INO1* gene in a *snf1* mutant strain of *Saccharomyces cerevisiae*. *Mol Cell Biol* **21:** 5710–5722

Stark C, Breitkreutz BJ, Reguly T, Boucher L, Breitkreutz A, Tyers M (2006) BioGRID: a general repository for interaction datasets. *Nucleic Acids Res* **1:** D535–D539

Styczynski MP, Moxley JF, Tong LV, Walther JL, Jensen KL, Stephanopoulos GN (2007) Systematic identification of conserved metabolites in GC/MS data for metabolomics and biomarker discovery. *Anal Chem* **79:** 966–973

Unnikrishnan I, Miller S, Meinke M, LaPorte DC (2003) Multiple positive and negative elements involved in the regulation of expression of *GSY1* in *Saccharomyces cerevisiae*. *J Biol Chem* **278:** 26450–26457

Usaite R, Nielsen J, Olsson L (2008a) Physiological characterization of glucose repression in the strains with *SNF1* and *SNF4* genes deleted. *J Biotechnol* **133:** 73–81

Usaite R, Patil KR, Grotkjær T, Nielsen J, Regenberg B (2006) Global transcriptional and physiological responses of *Saccharomyces cerevisiae* to ammonium, L-Alanine, or L-Glutamine Limitation. *Appl Microbiol Biotechnol* **72:** 6194–6203

Usaite R, Wohlschlegel J, Venable JD, Park SK, Nielsen J, Olsson L, Yates III JR (2008b) Characterization of global yeast quantitative proteome data generated from the wild type and glucose repression *Saccharomyces cerevisiae* strains: the comparison of two quantitative methods. *J Proteome Res* **7:** 266–275

Van Dijken JP, Bauer J, Brambilla L, Duboc P, Francois JM, Gancedo C, Giuseppin ML, Heijnen JJ, Hoare M, Lange HC, Madden EA, Niederberger P, Nielsen J, Parrou JL, Petit T, Porro D, Reuss M, van RN, Rizzi M, Steensma HY *et al* (2000) An interlaboratory comparison of physiological and genetic properties of four *Saccharomyces cerevisiae* strains. *Enzyme Microb Technol* **26:** 706–714

Venable JD, Wohlschlegel J, McClatchy DB, Park SK, Yates III JR (2007) Relative quantification of stable isotope labeled peptides using a linear ion trap-orbitrap hybrid mass spectrometer. *Anal Chem* **79:** 3056–3064

Villas-Boas SG, Hojer-Pedersen J, Akesson M, Smedsgaard J, Nielsen J (2005a) Global metabolite analysis of yeast: evaluation of sample preparation methods. *Yeast* **22:** 1155–1169

Villas-Boas SG, Moxley JF, Akesson M, Stephanopoulos G, Nielsen J (2005b) High-throughput metabolic state analysis: the missing link in integrated functional genomics of yeasts. *Biochem J* **388**(Part 2)**:** 669–677

Vincent O, Townley R, Kuchin S, Carlson M (2001) Subcellular localization of the Snf1 kinase is regulated by specific beta subunits and a novel glucose signaling mechanism. *Genes Dev* **15:** 1104–1114

Washburn MP, Wolters D, Yates III JR (2001) Large-scale analysis of the yeast proteome by multidimensional protein identification technology. *Nat Biotechnol* **19:** 242–247

Wiatrowski HA, Carlson M (2003) Yap1 accumulates in the nucleus in response to carbon stress in *Saccharomyces cerevisiae. Eukaryot Cell* **2:** 19–26

Wodicka L, Dong H, Mittmann M, Ho MH, Lockhart DJ (1997) Genome-wide expression monitoring in *Saccharomyces cerevisiae. Nat Biotechnol* **15:** 1359–1367

Young ET, Dombek KM, Tachibana C, Ideker T (2003) Multiple pathways are co-regulated by the protein kinase Snf1 and the transcription factors Adr1 and Cat8. *J Biol Chem* **278:** 26146–26158

Young ET, Kacherovsky N, Van RK (2002) Snf1 protein kinase regulates Adr1 binding to chromatin but not transcription activation. *J Biol Chem* **277:** 38095–38103